Acta Physica Academiae Scientiarum Hungaricae, Tomus 47 (1—3), pp. 209—217 (1979)

STRUCTURE OF $PbO-B_2O_3-Fe_2O_3$ MELTS

By

Á. VÉRTES

CENTRAL RESEARCH INSTITUTE FOR PHYSICS, HUNGARIAN ACADEMY OF SCIENCES
BUDAPEST, HUNGARY

The analysis of the mathematical model of liquid phase epitaxial crystal growth has drawn attention to the relationship between the growth process and the structure of high temperature solutions. Parameters in the model are not fully reported in the literature and even ionic equilibria are unknown for the $PbO-B_2O_3-Fe_2O_3$ system which is the preferred solvent for magnetic bubble storage technology.

Electric conductivity measurements relating to the ionic equilibria are described and a relationship is derived between composition dependence of activation energies and possible polyion formation. The suppositions below are supported by experiments:

$$PbO = Pb^{2+} + O^{2-}$$

$$B_2O_3 + 3\,O^{2-} = 2\,BO_3^{3-}$$

$$Fe_2O_3 + 3\,O^{2-} = 2\,FeO_3^{3-}$$

Equilibria are controlled by oxide-ion activity; a decrease in O^{2-} activity leads to the polymerization of oxianions. This model enables us to suggest as a general form

$$3\,YO_3^{3-} + 5\,FeO_3^{3-} = Y_3Fe_5O_{12} + 12\,O^{2-}$$

for the surface integration step of YIG.

Introduction

In the past few years the use of PbO-based high temperature solutions has become increasingly widespread. The method of liquid phase epitaxy (LPE) [1] has become an important part of the technology of magnetic bubble domain based mass storage devices. The epitaxial growth of YIG-type magnetic garnets on a nonmagnetic gallium-gadolinium-garnet (GGG) substrate takes place in a supercooled high temperature solution. In most of the technologies the defect-free substrate is horizontally rotated. In the development of the technology the importance of the knowledge of the growth kinetics became rapidly clear.

GHEZ and GIESS [2] proposed a theoretical model for the growth rate which consists of two steps. First, the crystal constituents diffuse through the boundary layer to the rotating disc; secondly, they take part in a surface integration step which is described as a first order chemical reaction. This model gives the time dependence of the growth rate in the following form:

$$V_g(t) = \frac{D(c_L - c_e)}{\varrho'\delta}\left[\frac{1}{1+R} + 2\sum_{n=1}^{\infty}\frac{\exp\left(-\alpha_n^2 Dt/\delta^2\right)}{1+R+R^2\alpha_n^2}\right], \qquad (1)$$

where δ is the width of the boundary layer, D is the diffusion constant, k is the kinetic coefficient for the surface reaction, $R = D/(\delta, k)$, ϱ' is the density of the crystal, c_L, c_e are the real and equilibrium concentrations of the solution, respectively, α_n-s are the roots of the equation: $\tan \alpha + R\alpha = 0$. The width of the boundary layer is obtained from hydrodynamic calculations:

$$\delta = 1.6 D^{1/3} \eta^{1/6} \varrho^{-1/6} r^{-1/2}, \tag{2}$$

where η is the viscosity, ϱ is the density of the melt, r is the rate of the rotation.

Let us see which material parameters are involved in the model of GHEZ and GIESS. The width of the boundary layer depends on D, η and ϱ, the growth process is governed by D, k, ϱ' and c_e. In the usual kinetic experiments η, ϱ, ϱ' and c_e are supposed as being known from other measurements, while the diffusion and kinetic coefficients are determined as regression parameters. However, these estimated values seem to be valid only with regard to the order of magnitude [2, 3]. It was because of these uncertainties that they decided to analyse the model [4]. The main problems are related to the characteristics of the surface integration step, to the influence of the heat of crystallization, and to the neglect of convective transport. On the other hand the structure and transport properties of the melt phase should be studied.

The investigations can be divided into two groups. The first is based on the measurement of the LPE growth kinetics as a function of supercooling, growth temperature, rotation rate and orientation of the substrate [5, 6]. The results give direct information on the applicability of the model and on the validity of its assumptions. The other group concerns the physico-chemical investigation of the high temperature solution, where special interest is devoted

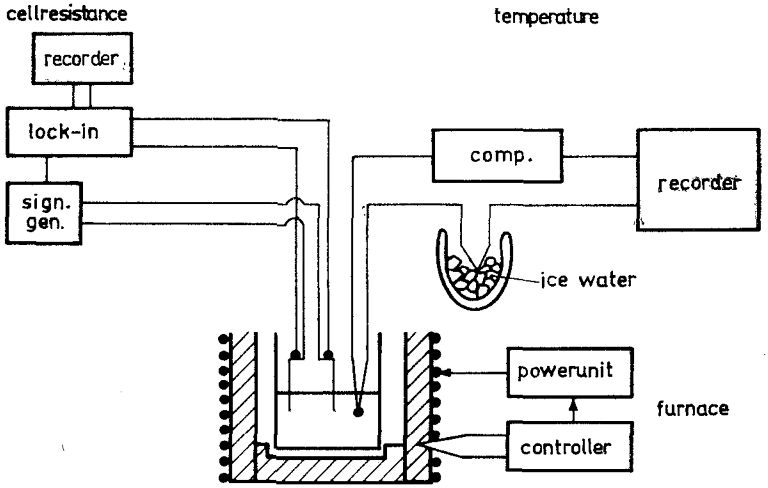

Fig. 1. Block scheme of experimental setup

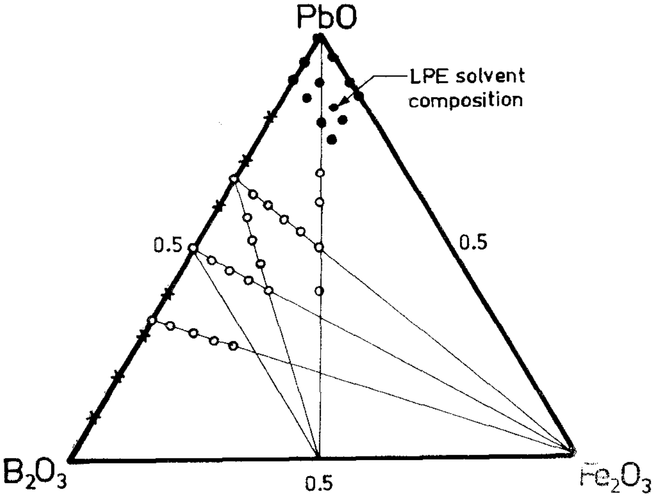

Fig. 2. Earlier measurements in the PbO—B_2O_3—Fe_2O_3 system [8—10] are characterized by much higher B_2O_3 content than in the LPE solvent (—➤). The compositions investigated by HIRASHIMA and YOSHIDA [8] (○) compared with our measurements (●)

to the diffusion constants of the components, the viscosity of the melt and to the solute — solvent interactions.

Our investigations are restricted to this second type of approach and to the PbO—B_2O_3—Fe_2O_3 ternary system.

Electric conductivity measurements

In order to describe the LPE growth process independent values of diffusion and kinetic coefficients are needed. Thus the question arises as to the real form of the crystal constituents in the melt. In other words: What types of ionic equilibria exist in the system? Earlier investigations of PbO—B_2O_3—Fe_2O_3 melts were focussed on the B_2O_3 rich glass forming region. The LPE solvent contains PbO as its main component and not more than 20 mol% of the other two oxides.

Experimental

The experimental setup (Fig. 1) is based on the AC voltage-drop method. The constant current driven by a current generator has 1 mA amplitude and 1 kHz frequency (it was earlier verified that this frequency is high enough to avoid the effects of electrode polarization). The voltage-drop is measured by a lock-in amplifier with potential wires leading directly to the electrodes. Two special requirements were taken into acount in the cell con-

struction: the extremely strong corrosiveness and the relatively high conductivity of the lead oxide. Frequency and geometrical characteristics of the cell were also investigated and optimized.

Fig. 2 shows the composition range of earlier measurements in the system [7—9] compared with ours. The result of Hirashima and Yoshida [7—9] relate to glass technology, therefore their compositions are on the B_2O_3 rich side.

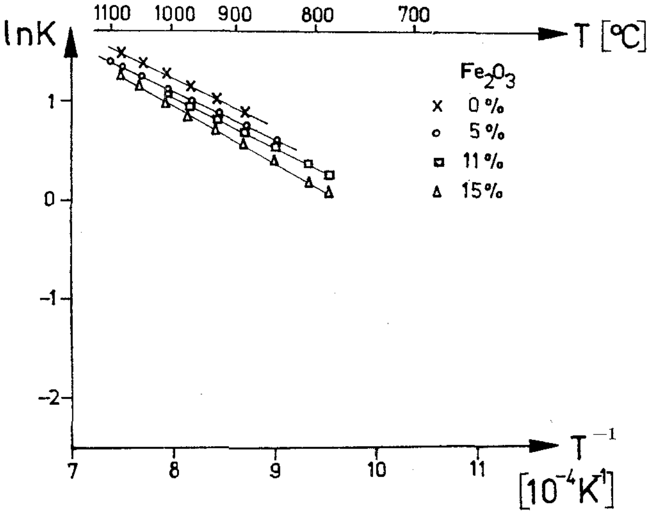

Fig. 3. Temperature dependence of electric conductivity in PbO—Fe_2O_3 systems

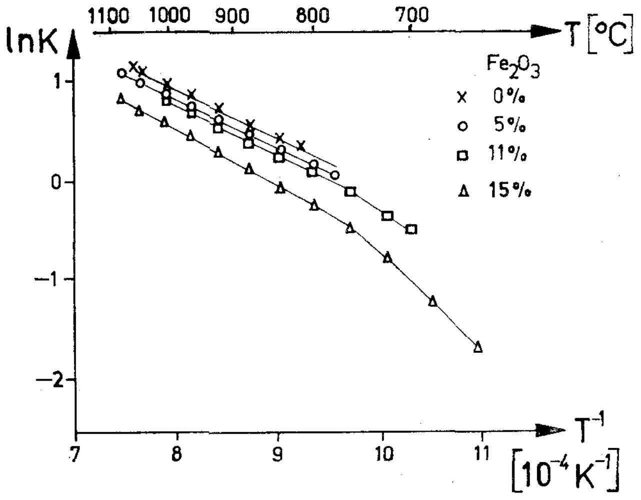

Fig. 4. Temperature dependence of electric conductivity in $(94-x)\%$ PbO — 6% B_2O_3 — $x\%$ Fe_2O_3 system. The slope of the curve of 15% Fe_2O_3 is not constant.

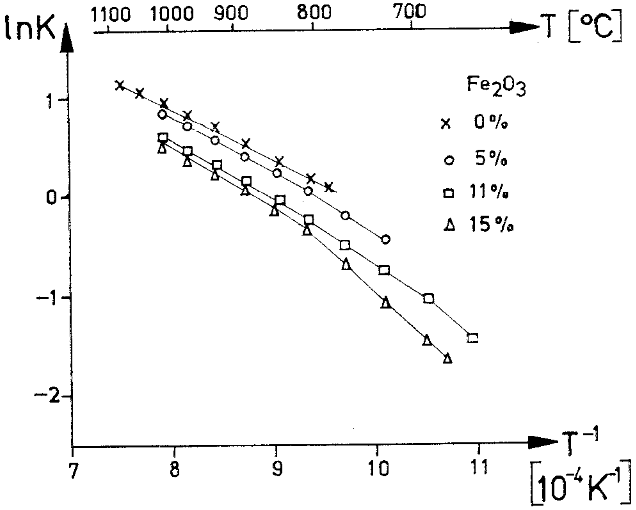

Fig. 5. Temperature dependence of electric conductivity in $(90-x)\%$ PbO — 10% B_2O_3 — $x\%$ Fe_2O_3 systems. In systems containing Fe_2O_3 the slopes of the curves are not constant.

The temperature dependence of specific conductivities on different compositions is shown in Figs. 3, 4 and 5 in Arrhenius-type plots. Activation energies (Figs. 6 and 7) are worked out by linear regression. It can easily be seen that the slope of the curves at high Fe_2O_3 content is not constant. This is probably due to the deviations described by ANGELL [10] but, in the absence of appropriate glass transition temperatures, we were not able to use his approximation.

Discussion

The interpretation of such measurements is usually made in a qualitative way, although there is a relation between the size of ions r_i and the equivalent conductance Λ. Let us combine the Stokes—Einstein and the Nernst equations:

$$\Lambda = \frac{F^2}{3N\pi\eta} \sum_i \frac{z_i x_i}{r_i}, \tag{3}$$

where N is the Avogadro number, F is the Faraday constant, z_i is the charge, r_i is the radius, x_i is the molar ratio of the i-th ion. This formula of course includes the approximations applied in the derivation of the Stokes—Einstein and Nernst equations. However, it is suitable as a means of explaining the effect of changing the composition. The appearance of new components has a direct influence by altering the $\sum_i z_i x_i/r_i$ sum and an indirect effect by changing the viscosity.

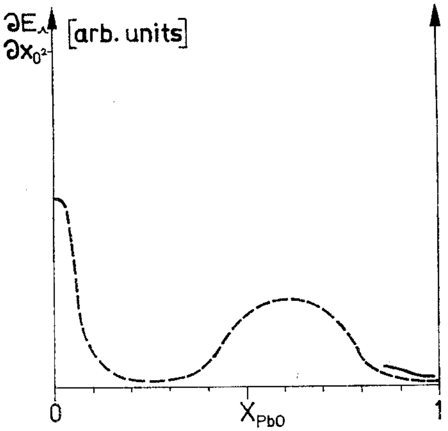

Fig. 6. Composition derivative of activation energies as a function of composition in PbO—B_2O_3 - - - and PbO—Fe_2O_3 —— systems. The "peaks" are due to polyion formation

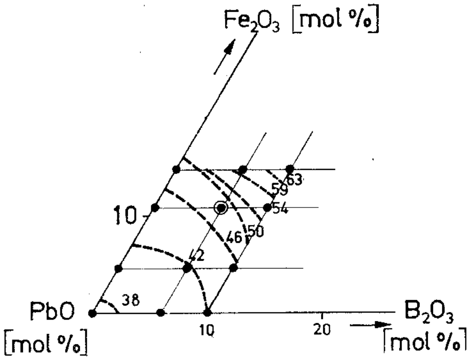

Fig. 7. Composition dependence of E_Λ in the ternary system. Equi-activation energy curves are indicated by dashed lines. The values are in kJ/mole. The composition indicated by a circle is due to the LPE solvent

In the case of polyion formation when n_i i-ions give n_j j-ions the change in the equivalent conductivity is:

$$\Lambda \frac{\partial \eta}{\partial x_i} + \eta \frac{\partial \Lambda}{\partial x_i} = \frac{F^2 n_i z_i}{3N\pi} \left(\frac{1}{r_j} - \frac{1}{r_i} \right), \tag{4}$$

where $n_j z_j = n_i z_i$ is involved because of charge conservation. This equation, in principle, gives the opportunity to make a rough estimation of the polyion size from $\Lambda(x_i)$, $\eta(x_i)$ data, but quantitative values have no real significance because of the approximations. Taking into account the Arrhenius type behaviour of the transport coefficients, one can obtain

$$\frac{\partial (E_\eta - E_\Lambda)}{\partial x_i} = \frac{n_i z_i}{\sum\limits_{l} \frac{z_l x_l}{r_l}} \left(\frac{1}{r_j} - \frac{1}{r_i} \right) - \frac{\partial \ln (\eta_0 \Lambda_0)}{\partial x_i}, \tag{5}$$

where E_A, E_η are the activation energies, A_0, η_0 are the pre-exponential factors. Thus the relation between the composition dependence of activation energies and the size of polyions becomes evident. In a rough approximation one can neglect the term containing the pre-exponentials and the effects of the viscosity deviation. In Fig. 6 the composition dependence of $\partial E_A/\partial x_{O^{2-}}$ is shown for the $PbO-B_2O_3$ and $PbO-Fe_2O_3$ binary systems according to our own and other [11] measurements. In the $PbO-B_2O_3$ system there are two composition ranges where structure changes may occur, viz. between 35 and 80 mol% PbO and between 0 and 10 mol% PbO. In the context of Eq. (4) it means that one can expect polyion formation in these regions. Following the assumptions of BOCKRIS [11] the first range is due to a chain-like polyborate anion formation whereas at the B_2O_3 rich end a polyion network formation takes place.

Pure lead oxide in the melt phase is assumed to be in a completely dissociated form. This is in accordance with the high values of its specific conductivity. The question is whether or not free electrons or holes take part in conduction. In other words: Is the lead oxide a liquid semiconductor? Although lead chalcogenides behave as semiconductors in the melt phase too [12]; conductivity determinations of PbO in the region of its phase transition supported the idea of ionic conduction. So the equilibrium:

$$PbO \rightleftharpoons Pb^{2+} + O^{2-} \qquad (6)$$

is moved almost completely to the right hand side.

The $PbO-B_2O_3$ system has been investigated over the whole composition range. Electrical conductivity measurements [11, 13, 14], EMF [15, 16] and calorimetric [17] investigations verify that with a value of less than 20 mol% B_2O_3 content, the O^{2-} ions — produced by complete dissociation of PbO — form monomer anions with the B_2O_3 in an acid-base equilibrium. The possible anions are BO_3^{3-} and perhaps BO_4^{5-}. In our range of interest the B_2O_3 content is lesss than 10 mol%, thus

$$B_2O_3 + 3\,O^{2-} \rightleftharpoons 2\,BO_3^{3-}. \qquad (7)$$

The activation energy of conductivity in $PbO-Fe_2O_3$ systems does not vary with the composition up to 15 mol% Fe_2O_3 (see Fig. 6). This makes it probable that Fe_2O_3 does not form polyions. However, a decrease in conductivity with increasing Fe_2O_3 content in Fig. 2 should in the spirit of Eq. (3) be related to the decrease in the number of O^{2-} ions and to the appearance of larger ions, respectively. So Fe_2O_3 seems to take part in the acid-base reaction:

$$Fe_2O_3 + 3\,O^{2-} \rightleftharpoons 2\,FeO_3^{3-} \qquad (8)$$

and to form the FeO_3^{3-} oxianion. The presence of FeO_3^{3-} ions is supported by the fact that $YFeO_3$ separates at much lower supercooling from the melt.

Activation energies for the ternary system are shown in Fig. 7 in the form of equi-activation energy lines. In the solvent region the lines go almost parallel with the straight lines of constant PbO content. This refers to the concept that B_2O_3 and Fe_2O_3 decrease the conductivity of PbO in a similar way. One can mention a sharp increase in activation energies above LPE solvent composition that is probably due to polyion formation.

Using this oxianion model one can suggest a similar mechanism for Y_2O_3 solvation in the form of YO_3^{3-} ions. The hypothesis is in good agreement with electrocrystallization experiments [18].

Another problem is the geometry of oxianions. The valence electron pair repulsion theory gives two versions: trigonal-planar and trigonal-pyramidal configurations [19]. To find the real geometry is far from our present possibilities.

The oxianion model has some consequences for the nature of the surface integration step, too. To understand the role of this reaction let us compare the coordination of metal atoms in the melt and in the crystal. The supposed trigonal-planar or trigonal-pyramidal geometry of the oxianions in the melt differ substantially from the octahedral coordination of metallic ions in the garnet crystal — as is known from X-ray diffraction measurements. This means that the torsion of bond angles during the integration is unavoidable. The formal equation prescribes bond breaking, too:

$$3\,YO_3^{3-} + 5\,FeO_3^{3-} = Y_3Fe_5O_{12} + 12\,O^{2-}. \tag{9}$$

This equation does not, of course, correspond to the real mechanism because of the low probability of coexistence of the large number of negative ions at the same place. However, it is useful to draw attention to the problem of O^{2-} accumulation and to its transport from the surface.

Acknowledgement

I am thankful to Dr. G. Konczos, Head of the Technological Department, Central Research Institute for Physics, Budapest, for his continuous help and interest in this work.

REFERENCES

1. D. Elwell and H. J. Schell, Crystal Growth from High Temperature Solutions, pp. 160—170, Academic Press, London, 1975.
2. R. Ghez and L. A. Giess, Mat. Res. Bull., **8**, 31, 1973.
3. S. Knight, B. S. Hewitt, D. L. Rode and S. L. Blank, Mat. Res. Bull., **9**, 895, 1974.
4. E. A. Giess and R. Ghez, Liquid Phase Epitaxy (in Epitaxial Growth, Ed. J. W. Matthews) Academic Press, London, 1975.
5. P. Görnert, S. Bornmann, F. Voigt and M. Wendt, Phys. Stat. Sol. (a), **41**, 505, 1977.
6. P. Görnert and S. Bornmann, Kristall und Technik, **13**, K41, 1978.
7. H. Hirashima and T. Yoshida, Yogyo-Kyokai-Shi, **79**, 316, 1971.
8. H. Hirashima and T. Yoshida, Xth International Congress on Glass, Kyoto, Japan, July, 1974.
9. H. Hirashima and T. Yoshida, Yogyo-Kyokai-Shi, **85**, 434, 1977.

10. C. A. Angell, J. Phys. Chem., **69**, 399, 1965.
11. J. O'M. Bockris and G. W. Mellors, J. Phys. Chem., **60**, 1321, 1956.
12. M. Cutler, Liquid Semiconductors, pp. 7., Academic Press, New York, 1977.
13. H. Hirashima and T. Yoshida, Yogyo-Kyokai-Shi, **82**, 30, 1974.
14. O. A. Esin and V. L. Ziaziev, Russ. J. Inorg. Chem., **2**, 1998, 1957.
15. M. L. Kapoor and M. G. Frohberg, Can. Met. Quart., **12**, 137, 1973.
16. B. M. Lepinskih and O. A. Esin, Russ. J. Inorg. Chem., **6**, 625, 1961.
17. J. L. Holm and O. J. Kleppa, Inorg. Chem., **6**, 645, 1967.
18. L. Jastrzebski, H. C. Gatos and A. F. Witt, J. Electrochem. Soc., **124**, 633, 1977.
19. R. J. Gillespie, Molecular Geometry, Van Nostrand Reinhold Co., London, 1972.